OPTIMUM RADIO TELESCOPE GEOMETRY

B. L. ULICH

NATIONAL RADIO ASTRONOMY OBSERVATORY

TUCSON OPERATIONS

INTERNAL REPORT NO. 2

SEPTEMBER 1976

OPTIMUM RADIO TELESCOPE GEOMETRY

B. L. Ulich

INTRODUCTION

This report is a brief summary of information available in the literature dealing with the electrical design of paraboloidal reflector antennas for use in radio astronomy. The first part deals with single parabolic reflectors used in the prime focus mode, and the second part deals with the classical paraboloidal/hyperboloidal Cassegrainian dual reflector system used at the secondary focus. In all telescope designs the optimum choice of reflector and feed geometry depends on the particular application for which the telescope is most often used. For example, the NRAO VLA antennas are composed of two "shaped" reflectors to achieve higher than normal axial gain by transforming the tapered feed illumination pattern into a more uniform amplitude across the primary aperture [1]. This is ideal for aperture synthesis observations but not for typical single dish work because of several other system degradations. First, the antenna sidelobe levels are increased considerably by the uniform aperture illumination, and this results in confusion for single beam observations. Second, the effects of coma are worse for a "shaped" reflector than for a classical Cassegrainian telescope. That is, the undistorted field of view is much smaller which limits how far the telescope can be beamswitched or how large a solid angle can be simultaneously imaged.

The most versatile design for single dish observations is the classical Cassegrain with a subreflector which can be conveniently removed for occasional prime focus detection. Access to the primary paraboloidal focus reduces the stringency of feed requirements and simplifies the use of incoherent, bolometric detectors at short millimeter wavelengths. In addition, future technological developments may lead to efficient two-dimensional detector arrays for imaging the entire field of view of the telescope rather than simply one point in the focal plane. Practical problems of operating large cryogenic detector arrays make the plate scale at the primary focus much more attractive for this purpose than the magnified plate scale at the secondary focus. It is clear, however, that for most receivers the secondary focus is preferable. First, access can be more convenient. Second, bulkier, heavier receivers can be mounted at the dish vertex than at the apex, and several receivers can be installed in a multi-pod arrangement. Third, the field of view of the Cassegrainian telescope is larger than at the primary focus, and thus comatic aberrations are smaller when beamswitching or scanning. Fourth, the feed spillover is now mainly directed at the cold sky rather than at the hot ground, and thus the antenna noise temperature is lower than that of the prime focus telescope.

The next sections of this report describe various figures of merit for the electrical performance of filled-aperture reflector antennas and how they are affected by the choice of telescope geometry.

PRIME FOCUS PARABOLOIDAL TELESCOPE

The reflecting telescope most often used in radio astronomy is the paraboloidal reflector with the receiver feed located at the primary focus. Figure 1 is a plot of the edge angle of the primary mirror as seen from the feed versus the focal length/diameter ratio (f/D) of the paraboloid [2]. Larger f/D values indicate small reflector edge angles. Typical radio astronomy antennas have values of f/D ranging from 0.25 to 0.8. If, for example, f/D = 0.43, then from Figure 1 the edge angle is 60° and the total angle subtended by the mirror is 120°.

The edge of a paraboloid is farther from its focus than is the reflector vertex, and, as a result, the $1/R^2$ variation in the feed power pattern with reflector distance produces additional tapering of the aperture illumination function. The resulting "space attenuation" is given in Figure 2 versus the f/D ratio of the paraboloid [2]. For an f/D = 0.43 the space attenuation is -2.5 dB at the edge of the reflector. In general, as the f/D decreases the reflector curvature increases and the magnitude of the space attenuation also increases. The space attenuation must be added to the feed power pattern to obtain the aperture illumination function, which can then be integrated to obtain the taper efficiency.

As a result of the curvature of the reflector an angular feed deflection results in an angular beam shift which is smaller by the beam deviation factor BDf [3]. Figure 3 is a plot of BDf versus f/D for an assumed feed edge illumination taper of -10 dB. As f/D increases the reflector becomes

flatter and the beam deviation factor approaches unity. For example, with an f/D = 0.43, the BDf = 0.84 but for f/D = 0.8, the BDf = 0.94. A lateral displacement of the feed away from the axis of the paraboloid results in a tilt of the beam in the opposite direction, a decrease in the antenna gain, an increase in the half-power beamwidth, and an increase in the level of the sidelobe nearest the reflector axis (coma lobe). One convenient criterion for judging the effect of coma is a -1 dB reduction in peak antenna gain (the Rayleigh limit). Figure 4 gives the number of half-power beamwidths scanned laterally off-axis for a -1 dB peak gain reduction versus reflector f/D [3]. It can be seen that the one-dimensional field of view increases approximately as $(f/D)^2$ and that the two-dimensional field of view increases as $(f/D)^4$. Thus flat, long-focal-length reflectors (large f/D) have larger fields of view and are much more efficient for scanning or imaging applications than shorter focal length systems. For example, an f/D = 0.43 reflector can scan only ±4 beamwidths for a -1 dB gain reduction, but an f/D = 0.8 reflector can scan about ±15 beamwidths.

Axial feed displacements decrease the peak gain, increase the half-power beamwidth, and increase the sidelobe levels. Figure 5 is a plot of the axial defocusing in wavelengths which results in -1 dB gain reduction versus reflector f/D [4]. A parabolic illumination function has been assumed. As f/D increases the focus curve broadens and the axial defocusing for a -1 dB gain reduction increases. Thus it appears that the mechanical tolerances of the feed position with long focal length reflectors are more lenient, and thus large f/D values are to be preferred since the

gain is less sensitive to defocusing. However, gravitational and thermal deformations of the reflector affect the axial focus position differently depending on the f/D. Figure 6 is a plot of the maximum reflector rim deflection in wavelengths for a -1 dB gain reduction versus f/D. Here a parabolic structural deformation has been assumed which changes the effective focal length of the primary mirror and thus decreases the gain. From Figure 6 it can be seen that for values of f/D <0.4 there is some advantage in smaller f/D ratios since structural deformations have a smaller effect on the gain. However, for values of f/D >0.4 surface deflections either parallel to the axis or normal to the reflector surface reduce the antenna gain by essentially a constant amount. Of course, deformations in the feed support legs will also defocus the feed and reduce the antenna gain. The feed movement will vary approximately linearly with f (and thus with f/D), and from Figure 5 one can deduce that the overall effect is that the gain of larger f/D antennas is slightly less sensitive to axial defocusing caused by changes in the length of the feed support structure. That is, the focus curve broadens faster than the focal length changes. Thus for most antennas the overall effect of structural deformations on the antenna gain due to axial defocusing is not highly sensitive to the reflector f/D.

For prime focus systems the feed mismatch reflection coefficient is small and not strongly dependent on f/D. Thus the feed reflection coeffient can be neglected in determining the optimum prime focus telescope geometry.

In addition, for large diameter (in wavelengths) antennas, the feed blockage is negligible and good feed taper, spillover, and phase efficiencies can be obtained for any value of f/D between 0.2 and 1.0 using simple waveguide horns.

Because of the curvature of the paraboloidal reflector, some of the power radiated by the feed will be converted into cross polarized radiation in the aperture plane. The result is reduced gain and increased sidelobe levels. The four main cross polarization lobes peak at the intersections of the first null in the principal polarization pattern with the four intercardinal planes, and their peak amplitudes are given in Figure 7 as a function of f/D [5]. As expected, the peak cross polarization lobe level increases with reflector curvature and thus with decreasing f/D. Thus larger f/D ratios are preferred to minimize the deleterious effects of cross polarization.

In this section the effects of changes in the focal length of a paraboloidal reflector on its electrical performance have been given. It seems clear that longer focal length radio telescopes (f/D = 0.6-0.8) are preferable since they have wider fields of view and are less affected by cross polarization. However, they are structurally larger and more expensive (especially if they require a larger diameter radome), and a compromise between antenna performance and cost must be reached in all cases depending on the detailed application of the telescope.

CASSEGRAINIAN TELESCOPE

The classical Cassegrainian telescope is comprised of a paraboloidal primary reflector of diameter D and focal length f and of a hyperboloidal secondary reflector of diameter d, magnification M, and with the secondary focus at a distance H above the vertex of the paraboloid. As previously mentioned, the Cassegrainian telescope has several advantages over the prime focus telescope: (1) more convenient receiver access, (2) usually greater equipment loading capacity, (3) wider field of view, and (4) lower antenna noise temperature. These advantages are not free, however, and are gained at the cost of a secondary reflector which has to have an RMS surface deviation at least a factor of 3 smaller than that of the primary mirror and also at the cost of larger diameter and longer feed horns.

Defocusing the subreflector axially produces a focusing curve which is only slightly narrower than the prime focus feed axial defocusing curve. Similarly, lateral subreflector shifts produce beam deviations which are only slightly smaller than in the prime focus feed case. Thus the mechanical tolerances on the subreflector position are nearly the same as for the prime focus feed, and the applicable comments in the previous section can also be applied to the position of the Cassegrainian secondary mirror. The Cassegrainian feed position is about M times less sensitive laterally and about M^2 times less critical axially than the prime focus feed position. Thus the two-dimensional field of view of the Cassegrainian telescope is

about M^2 times larger than at the prime focus, and greater freedom is allowed in locating Cassegrainian feed horns.

The presence of the subreflector produces central aperture blockage which reduces the antenna gain and increases the sidelobe levels. Figure 8 is a plot of the gain reduction versus the central blockage parameter $\delta = d/D$ for a -10 dB aperture illumination function [6]. Note that because of the amplitude taper a 1% area blockage in the center of the antenna reduces the gain by about 3%. Figure 9 is a plot of the first sidelobe level versus the central blockage parameter δ [4]. Each 1% area blocked in the dish center raises the first sidelobe by about 1.5 dB. Clearly, then, large diameter subreflectors will significantly degrade the antenna performance. Of course, Figures 8 and 9 can also be applied to prime focus telescopes where the radiometer box and feed horn block the primary mirror.

Decreasing the diameter of the subreflector will reduce the effects of central blockage, but if the diameter is made too small several other effects may also significantly affect the antenna performance. First, it becomes practically difficult to construct efficient feeds for very high magnification optics. Second, when the subreflector is a finite number of wavelengths in diameter, some power is lost due to edge diffraction. Figure 10 is a plot of the subreflector edge diffraction efficiency as a function of the subreflector diameter in wavelengths assuming a -10 dB illumination taper. A surprisingly large subreflector ($d/\lambda > 200$) is necessary to reduce the edge diffraction loss to less than 2%. Similarly, the large magnifications associated with small subreflectors increase the feed mismatch

reflection coefficient [7]. The power scattered from the subreflector back into the feed leads to a sinusoidal ripple in the frequency spectrum of the total received power which can seriously limit the quality of spectral line observations. Figure 11 is a plot of the peak-to-peak amplitude of this baseline ripple (expressed as a percentage of the average received power) versus δ for a Cassegrainian telescope with f/D = 0.43 and H = 0.4 m. The ripple amplitude decreases linearly with increasing subreflecotr diameter. Tunable matching devices such as a secondary vertex disk can be used to cancel the secondary reflection, but the necessary disk diameter varies with wavelength and a good match with a single disk can be achieved only over a small bandwidth.

Von Hoerner [8] has defined a maximum scanning angle for the Cassegrainian telescope based on the increase in spillover rather than on a gain reduction due to phase errors. This practical spillover limit results in a gain reduction of several percent and is more stringent than the phase error limit. The maximum off-axis scanning angle in half-power beamwidths is plotted in Figure 12 versus normalized subreflector diameter d/D for a primary reflector with f/D = 0.43 and H = 0.4 m. Two curves are given for λ = 1 mm and λ = 1 cm. The physical diameter of the Cassegrainian feed cluster which satisfies this limit is independent of wavelength, and thus the number of half-power beamwidths which can be scanned varies inversely with wavelength. At any give wavelength the maximum scanning angle varies approximately linearly with the subreflector diameter. The coma lobe level at the maximum scanning angle [8] is plotted in Figure 13 versus the normalized subreflector diameter assuming the same primary geometry used above. With larger subreflectors the coma lobe becomes

intolerably large and further limits the useful size of the feed cluster.

Nutating the subreflector provides a convenient method of beamswitching to cancel the background radiation. For maximum efficiency the moment of inertia of the subreflector should be as low as possible, which means a small lightweight mirror. In addition, some telescope pointing errors can be sensed and corrected in real time by appropriate subreflector motions [8]. These also require a servo control loop with wide bandwidth and fast response. Practically speaking, the smallest subreflector which meets the electrical performance criterea should be chosen to optimize the dynamical response.

The effects of cross polarization are generally negligible for Cassegrainian telescopes and need not be considered here. Similarly, for large wavelength aperture systems the minimum length of feed horns should not impose a lower limit on the subreflector size since short horns illuminating phase-error-correcting lenses may be used. Generally the overall axial length can be made as short as the lens diameter, and long high-gain horns are unnecessary at the Cassegrainian focus.

In this section the effects of basic Cassegrainian design parameters on the electrical performance of a telescope have been given, and comparisons have been made with prime focus paraboloidal reflectors. Cassegrainian systems offer several advantages for use in radio astronomy, but care must be exercised in the choice of the primary reflector f/D, the

location of the secondary focus, and the subreflector diameter in order to achieve the optimum performance. These choices will generally represent a telescope design which reasonably compromises the electrical performance to meet other requirements on the types of observations to be made, on the mechanical structure, and on the cost.

REFERENCES

[1] W. F. Williams, "High efficiency antenna reflector," Microwave J., vol. 8, pp. 79-82, July 1965.

[2] M. L. Meeks, Methods of Experimental Physics: Astrophysics, vol.12, part B: Radio Telescopes. New York: Academic Press, 1976.

[3] J. Ruze, "Lateral-feed displacement in a paraboloid," IEEE Trans. Antennas Propagat., vol. AP-13, pp.660-665, Sept. 1965.

[4] J. W. M. Baars, "Characteristics of the paraboloidal reflector antenna," National Radio Astronomy Observatory, Electronics Division Internal Report No. 57, Aug. 1966.

[5] J.W.M. Baars, "A comparison between prime focus and Cassegrain antennas," National Radio Astronomy Observatory, Internal Report, Oct. 1964.

[6] J. Ruze, "Feed support blockage loss in parabolic antennas," Microwave J., vol. 12, pp. 76-80, Dec. 1968.

[7] W.V.T. Rusch and P.D. Potter, Analysis of Reflector Antennas. New York: Academic Press, 1970.

[8] S. Von Hoerner, "The choice of a Cassegrain system for the 65-m telescope," National Radio Astronomy Observatory, Engineering Division Internal Report No. 31, Feb. 1970.

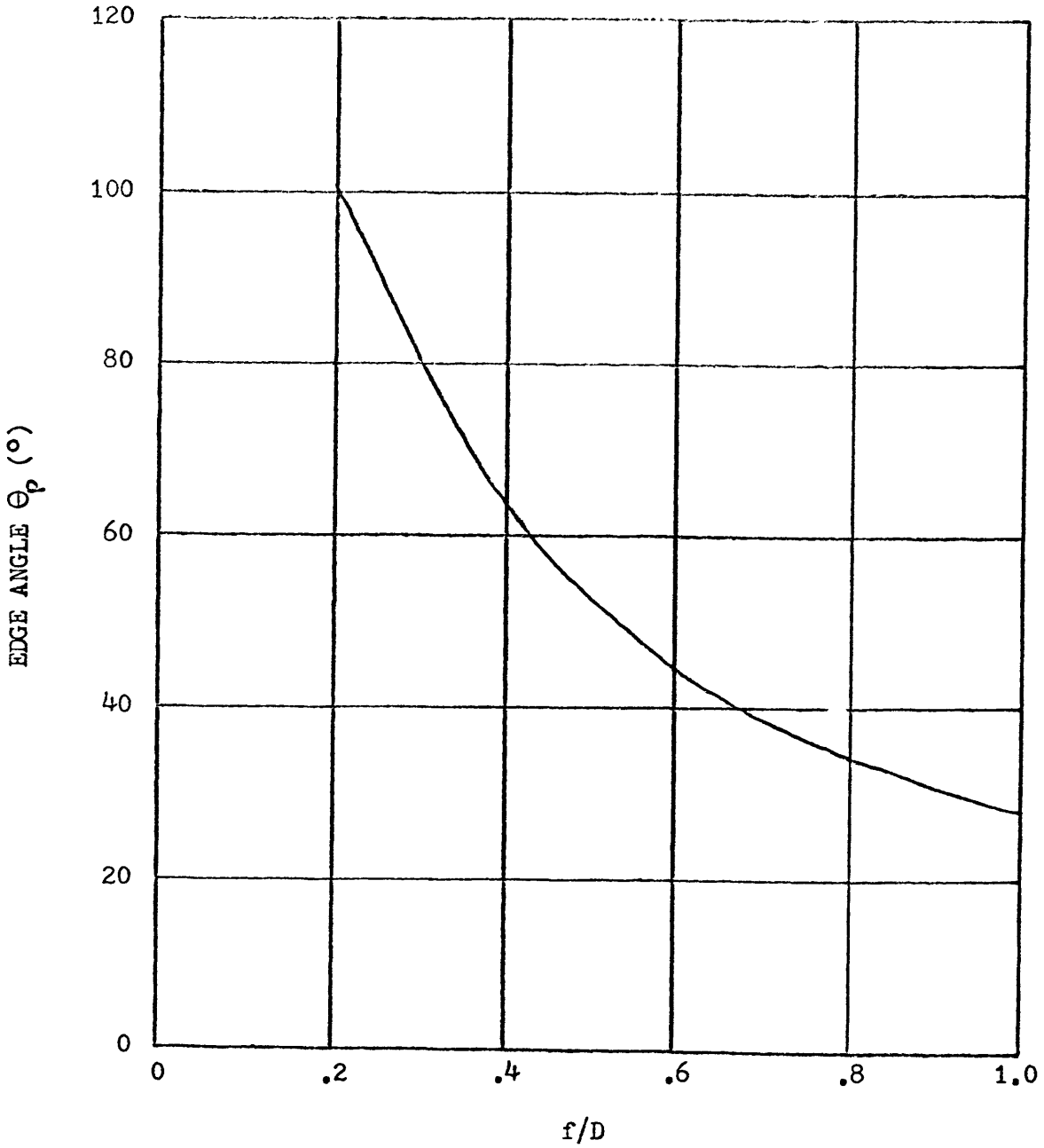

FIGURE 1 - Edge angle Θ_p of primary reflector as a function of f/D.

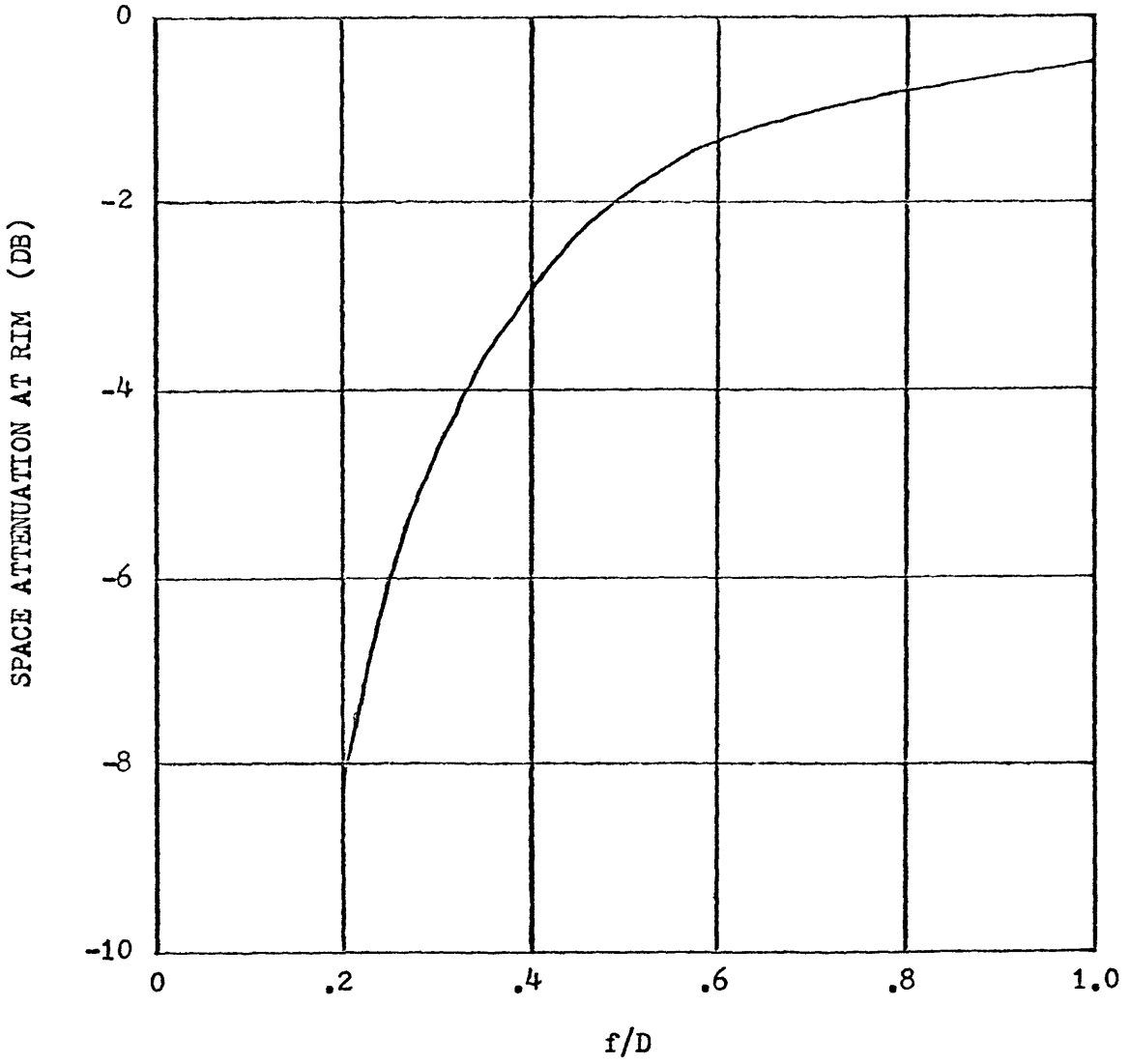

FIGURE 2 - Space attenuation as a function of primary reflector f/D calculated for the edge of the reflector.

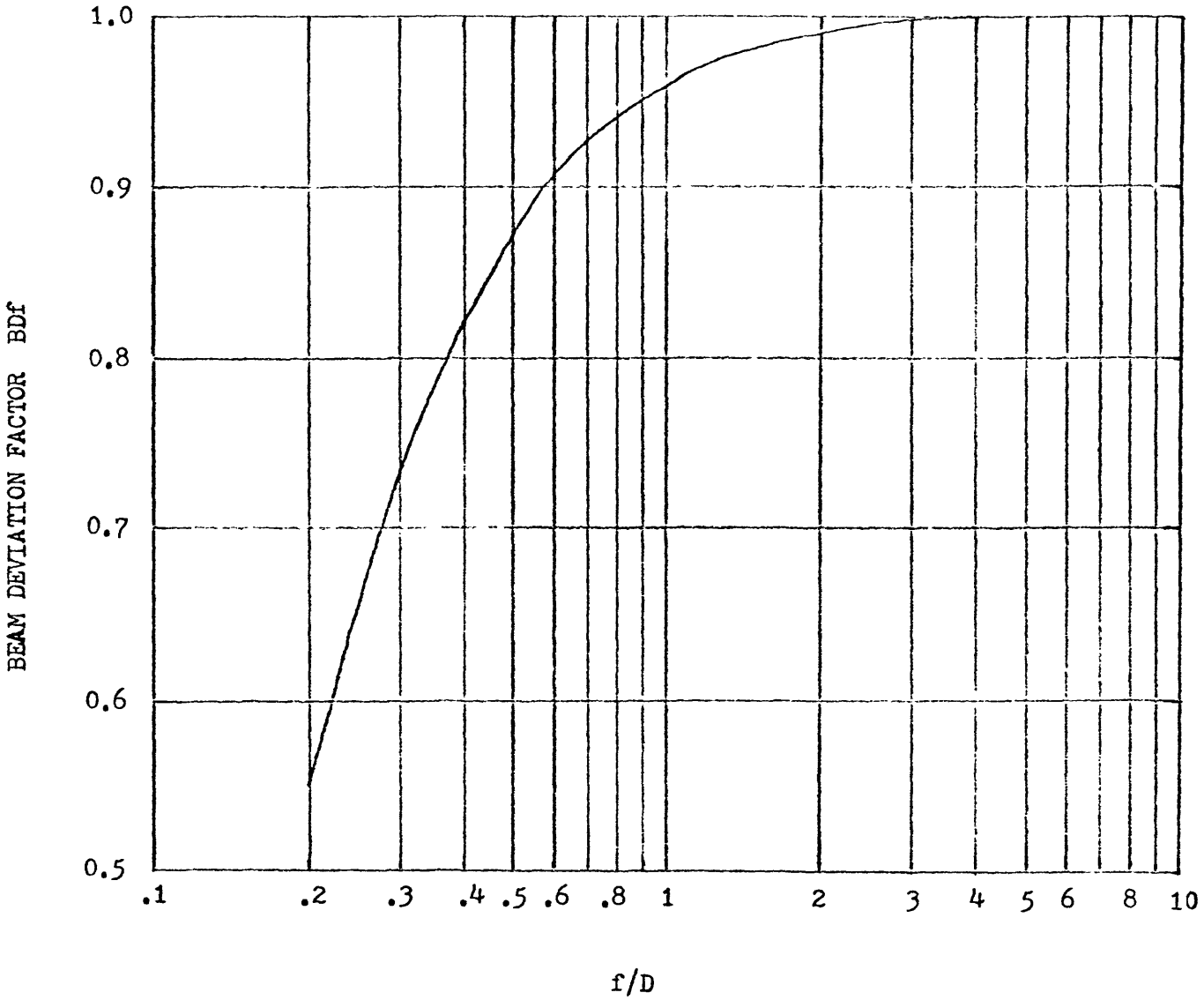

FIGURE 3 - Beam deviation factor BDf as a function of primary reflector f/D for feed edge illumination taper of -10 dB.

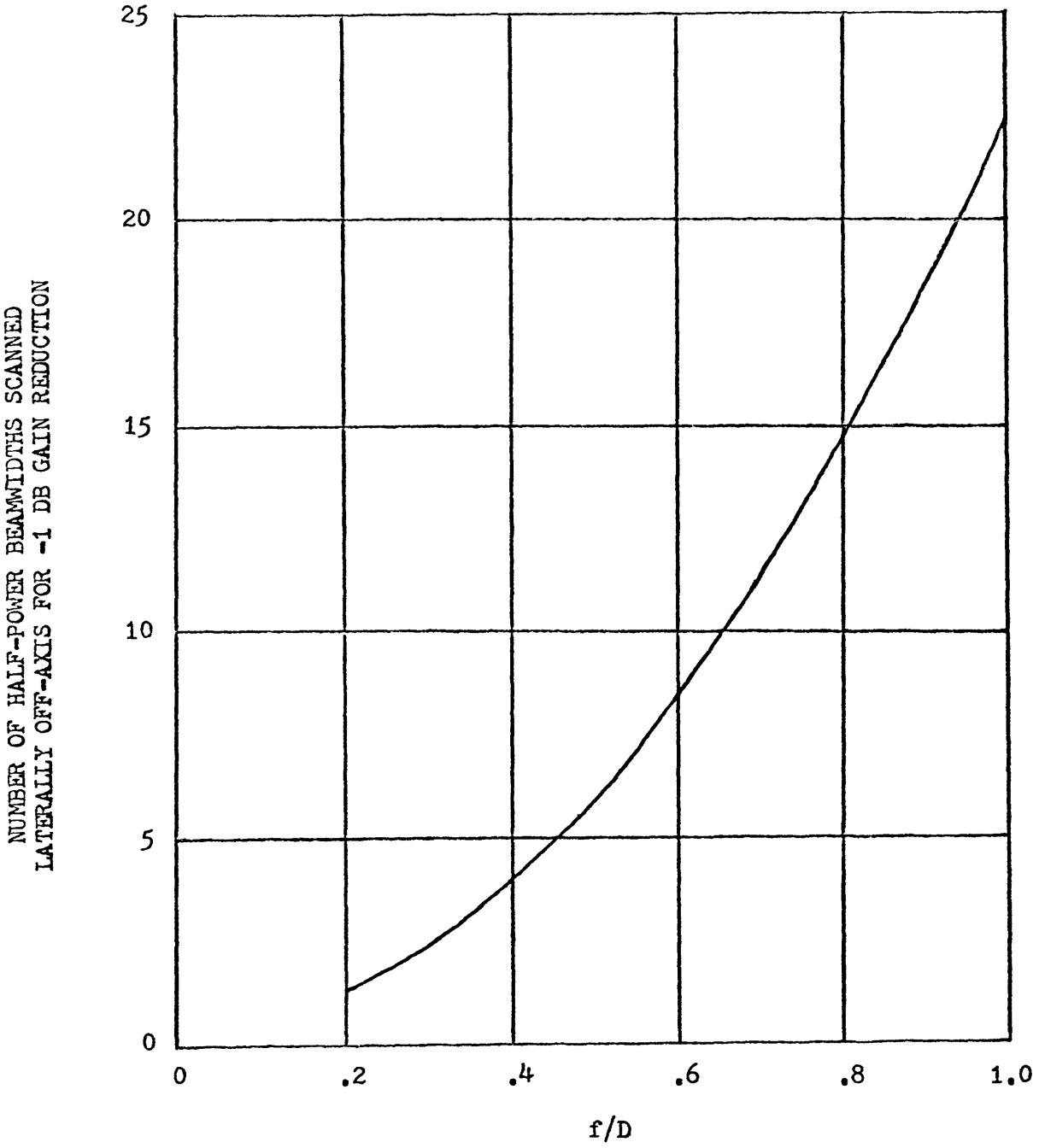

FIGURE 4 - Number of half-power beamwidths scanned laterally off-axis for -1 dB gain reduction as a function of primary reflector f/D.

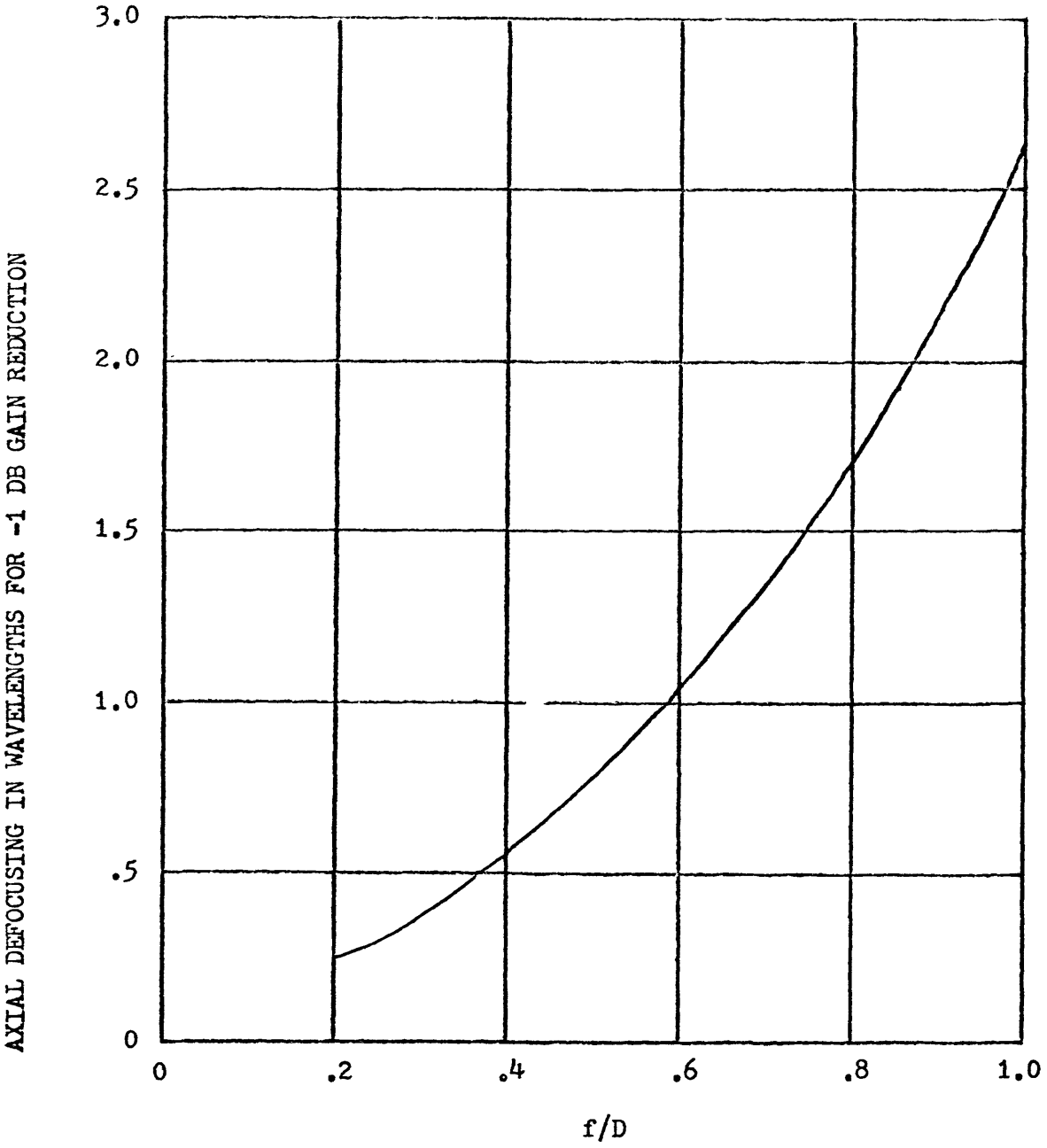

FIGURE 5 - Axial defocusing in wavelengths for -1 dB gain reduction as a function of primary reflector f/D.

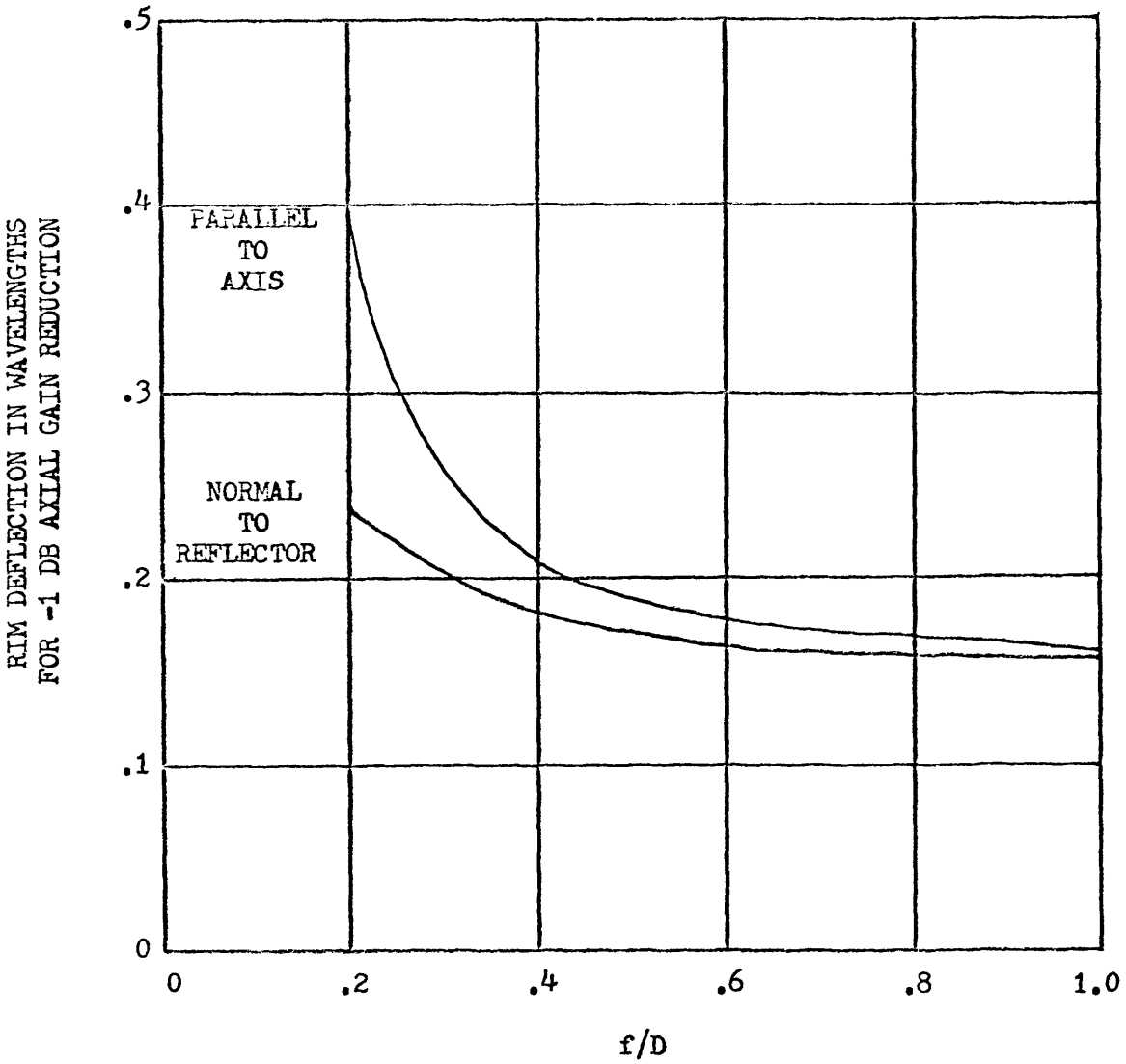

FIGURE 6 - Rim deflection in wavelengths for -1 dB axial gain reduction as a function of primary reflector f/D.

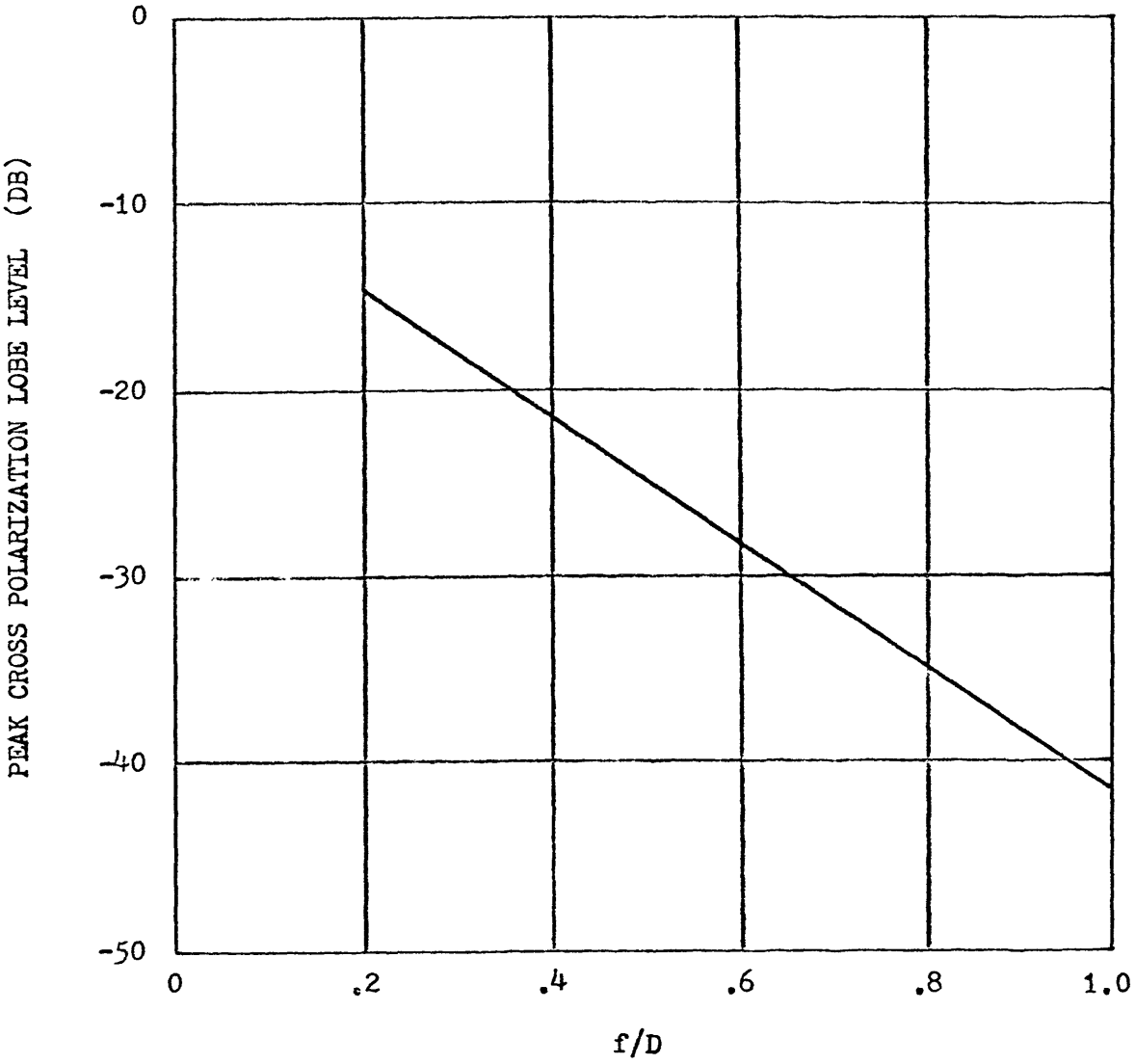

FIGURE 7 - Peak cross polarization lobe level as a function of the primary reflector f/D.

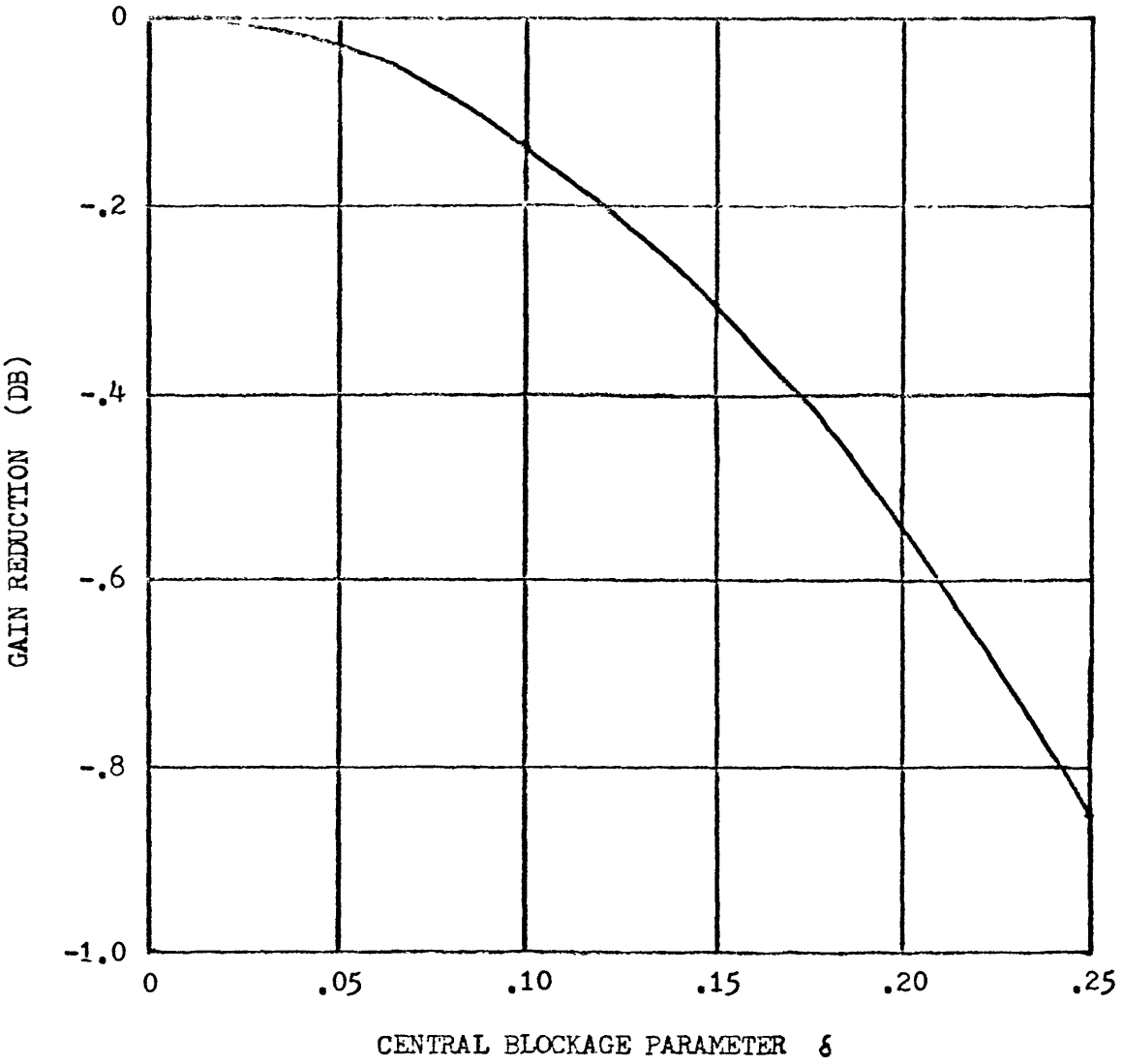

FIGURE 8 - Antenna gain reduction as a function of the central blockage parameter $\delta = d/D$.

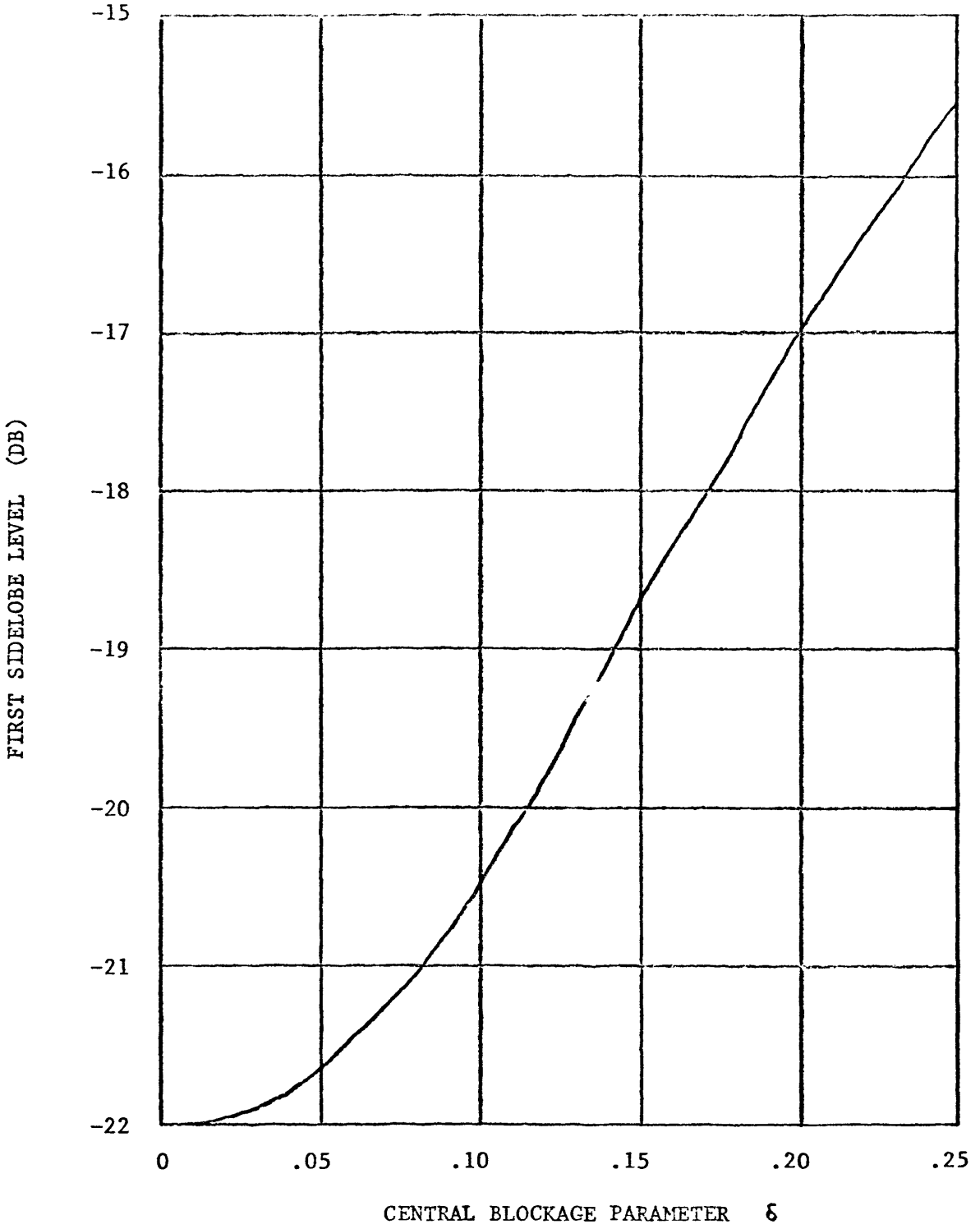

FIGURE 9 - First sidelobe level as a function of the central blockage parameter $\delta = d/D$.

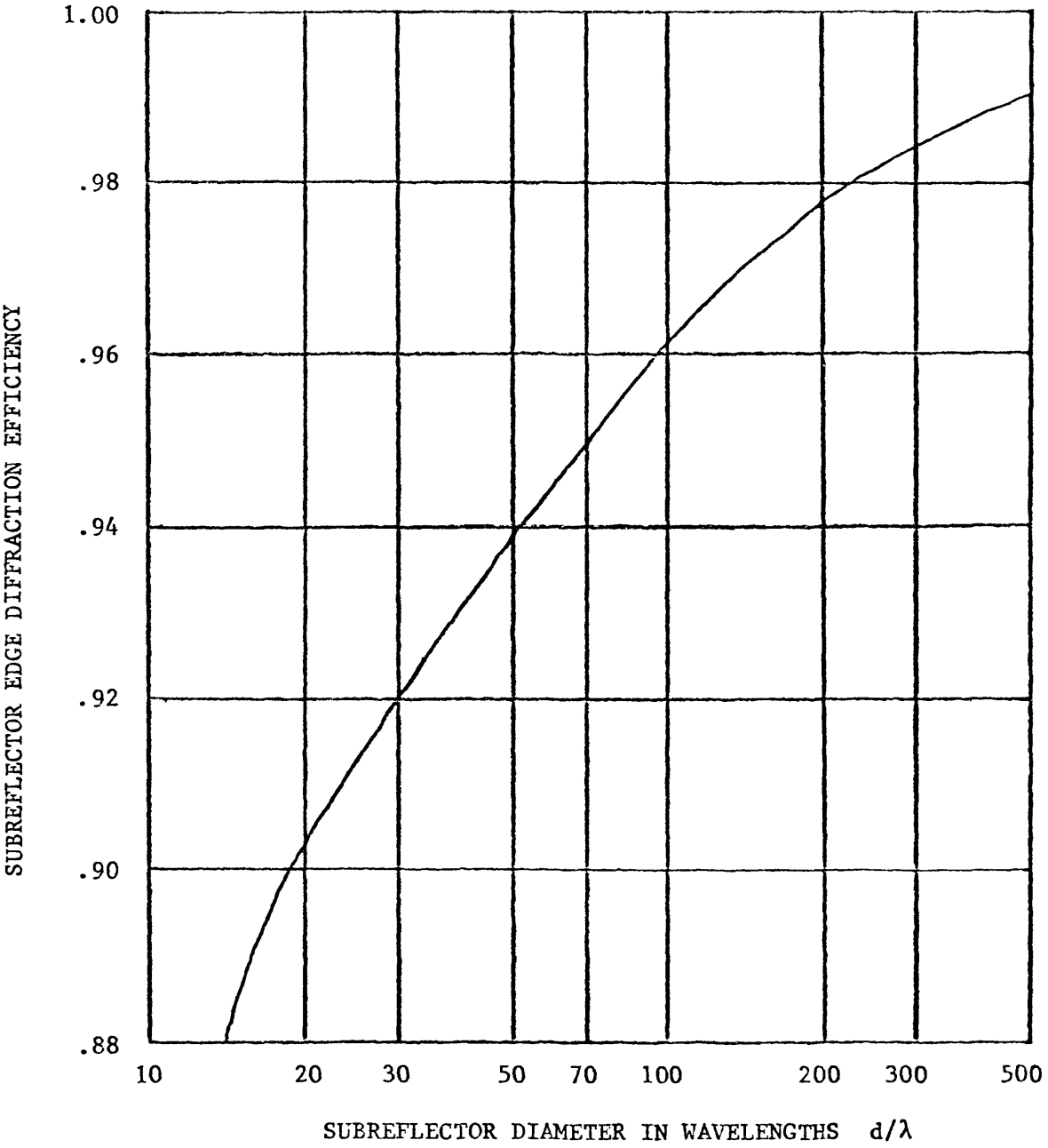

FIGURE 10 - Subreflector edge diffraction efficiency as a function of the subreflector diameter in wavelengths for a -10 dB illumination taper.

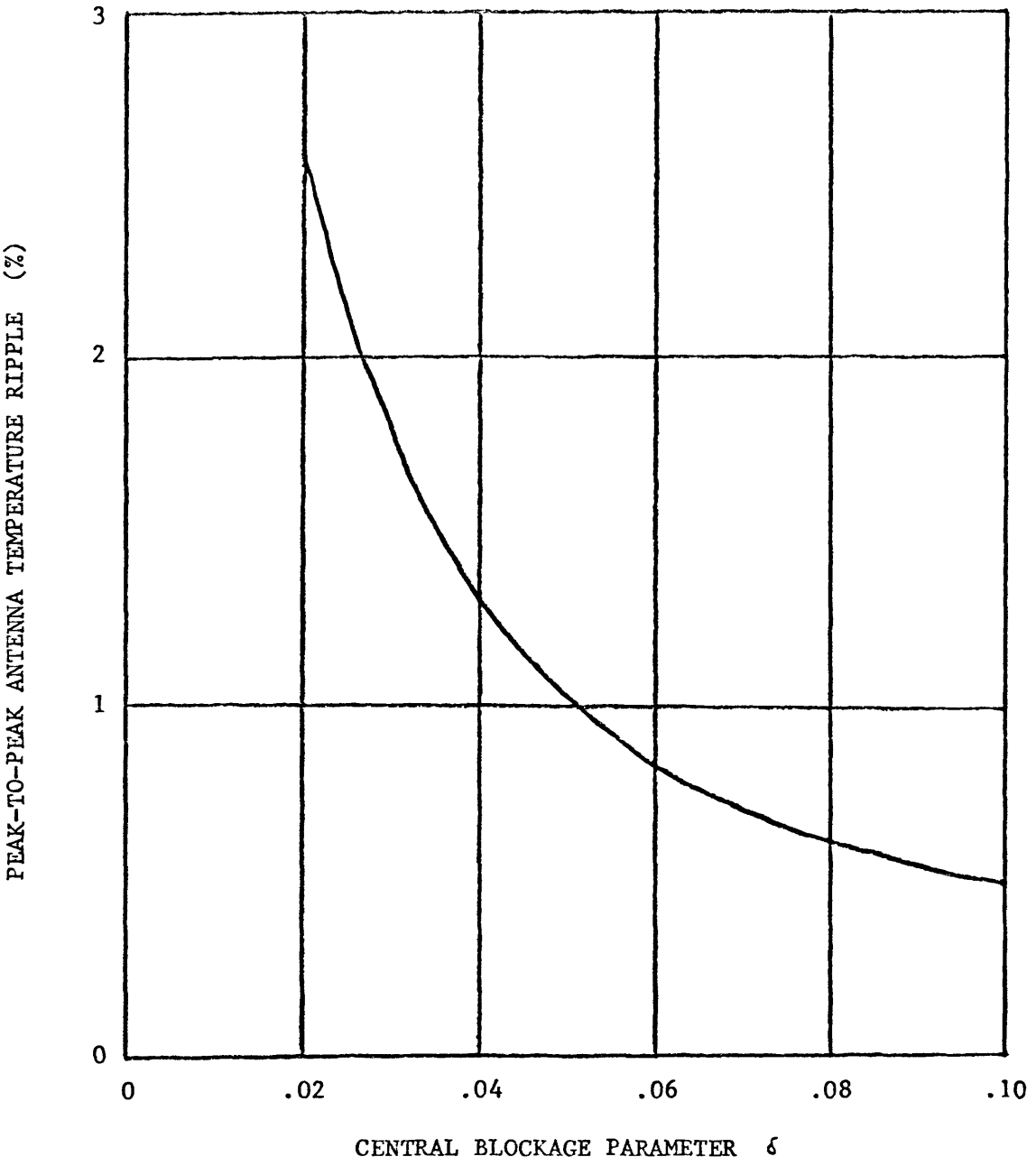

FIGURE 11 - Peak-to-peak antenna temperature ripple as a function of the central blockage parameter δ with f/D = 0.43 and H = 0.4 m.

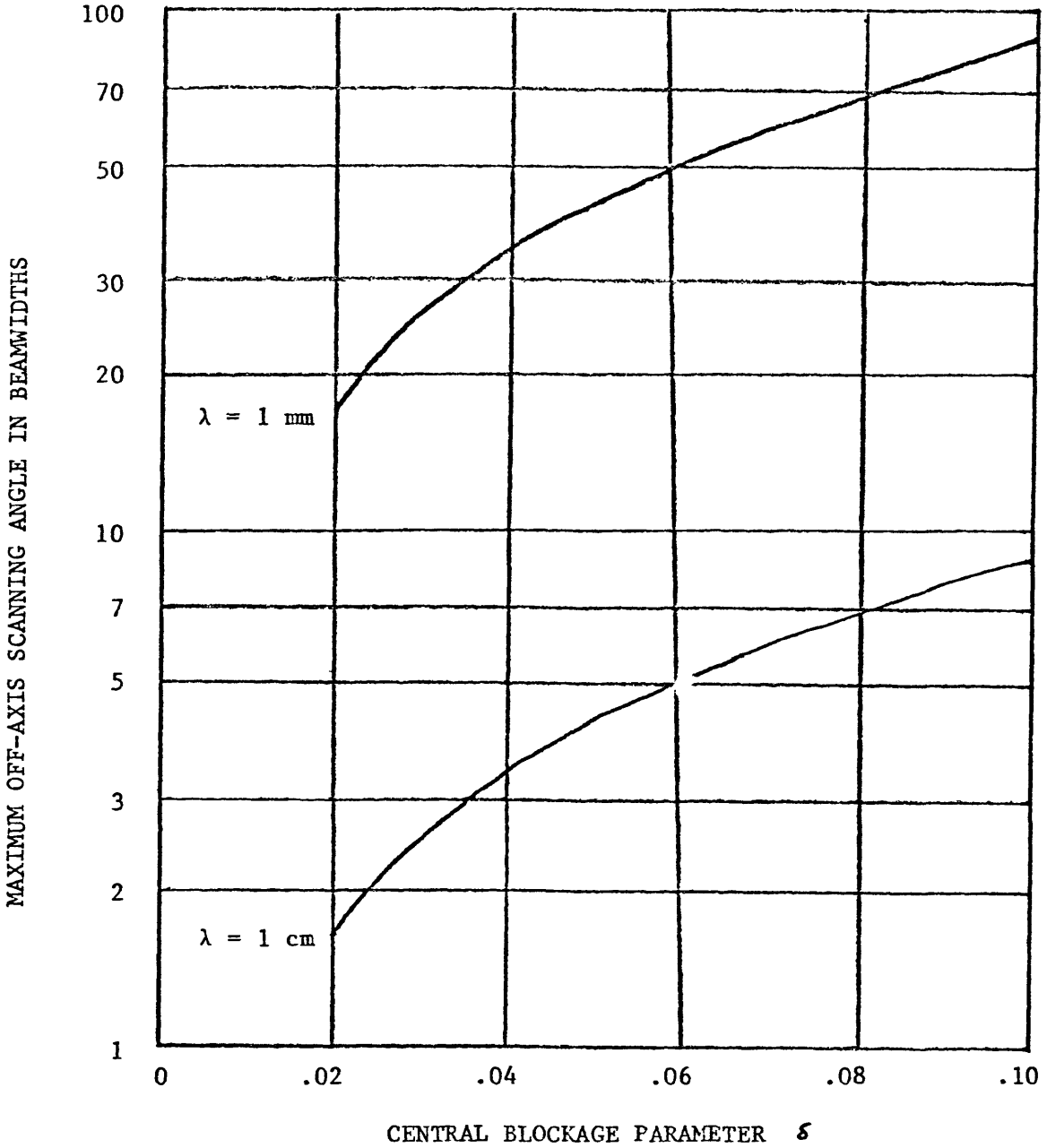

FIGURE 12 - Maximum off-axis scanning angle in half-power beamwidths as a function of the central blockage parameter $\delta = d/D$ with $f/D = 0.43$ and $H = 0.4$ m.

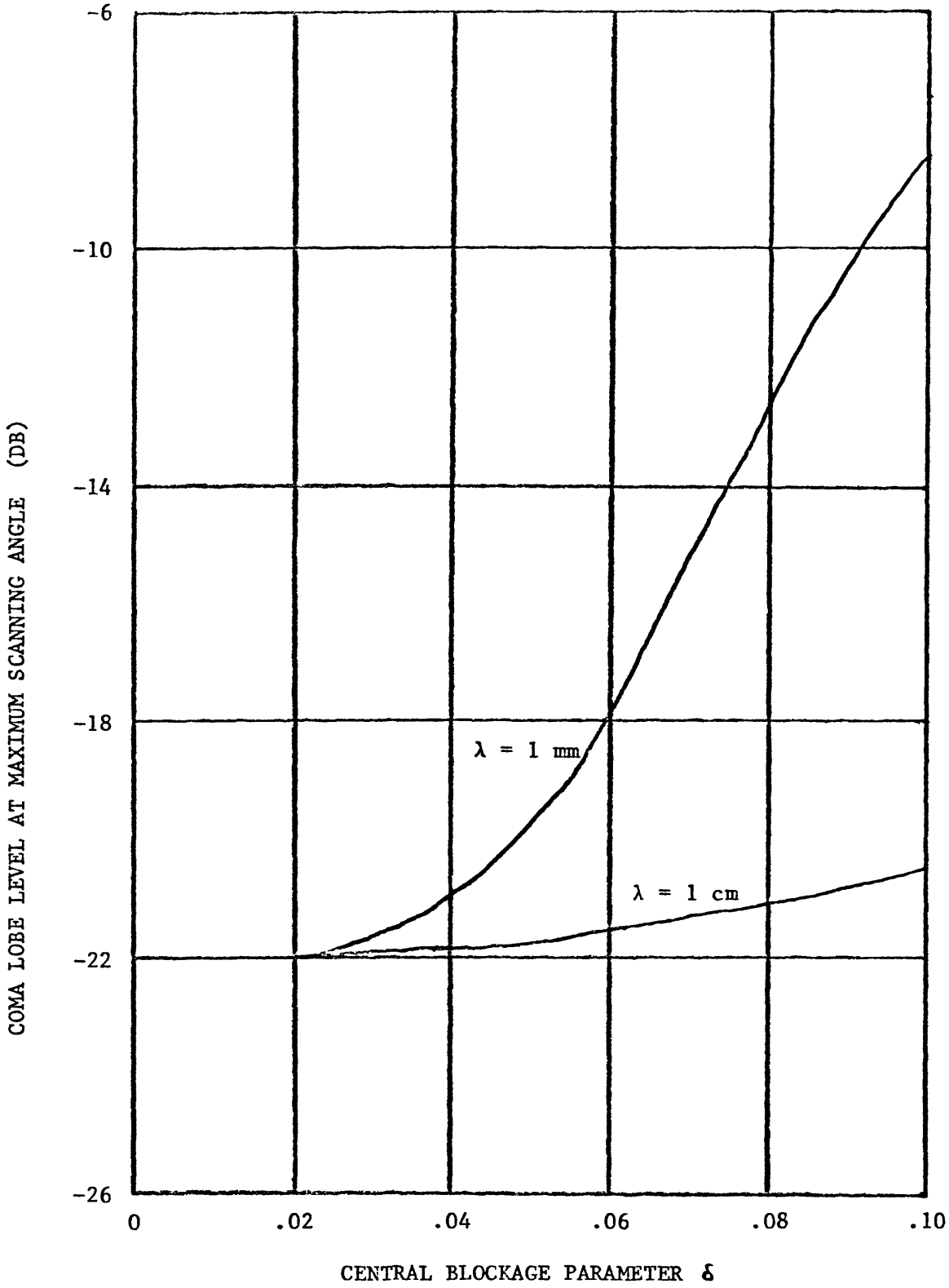

FIGURE 13 - Coma lobe level at maximum scanning angle as a function of the central blockage parameter $\delta = d/D$ with $f/D = 0.43$ and $H = 0.4$ m.